Ultrasonic guided waves measurements using Fiber Bragg Gratings on optical fibers under varying environmental conditions

Arnaud Recoquillay, Nicolas Roussel, Laurent Maurin, Guillaume Laffont, Bastien Chapuis

Proceedings of the ASME 2023
50th Annual Review of Progress in
Quantitative Nondestructive Evaluation
QNDE2023
July 24-27, 2023, Austin, Texas

QNDE2023-XXXXX

ULTRASONIC GUIDED WAVES MEASUREMENTS USING BRAGG GRATINGS ON OPTICAL FIBERS UNDER VARYING ENVIRONMENTAL CONDITIONS

Arnaud Recoquillay
Université Paris-Saclay, CEA, List, F-91120, Palaiseau, France

Nicolas Roussel
Université Paris-Saclay, CEA, List, F-91120, Palaiseau, France

Laurent Maurin
Université Paris-Saclay, CEA, List, F-91120, Palaiseau, France

Guillaume Laffont
Université Paris-Saclay, CEA, List, F-91120, Palaiseau, France

Bastien Chapuis
Université Paris-Saclay, CEA, List, F-91120, Palaiseau, France

ABSTRACT

Fiber Bragg Gratings (FBGs) are promising ultrasound transducers, especially for Structural Health Monitoring (SHM), since they can be seamlessly integrated into structures and multiplexed, and can also sustain harsh environments (extreme temperatures, radiations, electromagnetic environments…). However, their widespread use in ultrasonics has been limited until now because the sensitivity of the edge filtering technique, as implemented so far, is strongly impacted by environmental conditions such as temperature or deformation of the host structure, leading to a loss in sensitivity. We present here a solution enabling measurements under varying environmental conditions based on the low frequency tracking of the setting point in order to keep the sensitivity of this method at an acceptable level. The setup was successfully tested during the 4-points bending test of a composite panel at varying strain rates.

Keywords: ultrasound, fiber Bragg gratings, guided waves, structural health monitoring, environmental and operational conditions

1. INTRODUCTION

Ultrasonic guided waves are ultrasonic waves propagating in elongated structures such as plates, rails or tubes. They are propagating over large distances, making them an object of interest for nondestructive testing, in particular for Structural Health Monitoring (SHM) as this feature enables to use sparse arrays of sensors to cover large areas of a structure under monitoring. Their actuation and measurement can be performed using classic piezoelectric transducers, see [1][2] for example. However, there are some limitations to the use of these sensors for Structural Health Monitoring: they offer small integration capabilities as they can be rather bulky and need two wires per sensor, which in the end may amount to a lot of circuitry depending on the density of sensors and the size of the monitored structure. Furthermore, they are not suited for harsh environments such as extreme temperatures, electromagnetic environments or explosive atmospheres. To circumvent these issues, more and more studied monitoring solutions are based on optical fiber sensors. These sensors have proven efficient for many low frequency applications, based either on distributed [3] or local measurements [4]. Distributed acquisitions such as Distributed Acoustic Sensing [5] are limited in terms of sampling frequency and spatial resolution and are not suited, as of today, for ultrasonic measurements. On the other hand, local measurements using Fiber Bragg Gratings (FBGs) have been studied in the last decades for ultrasonic applications, and techniques such as “edge filtering” lead to promising results [6][7]. Contrary to classic piezoelectric transducers, these sensors are only able to detect waves. They are hence often studied coupled with an actuator. Another possibility is the use of passive data, that is the reconstruction of signals of interest from the measurement of ambient noise. This was done successfully in [8] for geophysics, that is at rather low frequencies, and then for ultrasonic frequencies in [9]. Imaging using conventional SHM algorithms using passive data on FBG was later obtained in [10].

These results using FBG transducers for ultrasonic measurements were however obtained in laboratory conditions, that is in controlled environmental and operational conditions (EOCs). In practice, it is well known

that FBG transducers are sensitive to strain and temperature, which can lead to the loss of the setting point in edge filtering when these parameters are varying. Some solutions exist to make the system resilient to these variations, but they either need some further assumptions, such as two FBGs subjected to the same EOCs [12] or ultrasonic waves [13], or are based on optical circuitry hindering the integration of the system [11].

The aim of this paper is to propose a solution similar to [14] enabling to track the setting point of an edge filtering FBG system under low frequency variations, typical of EOC variations, with a rather simple system, hence preserving its integration capabilities. The first section will describe the solution before showing its validation on a 4-points bending test.

2. ULTRASONIC MEASUREMENTS USING FIBER BRAGG GRATINGS UNDER DYNAMIC CONDITIONS

We describe here the technical solution developed to track the setting point of the edge filtering technique while environmental or operational conditions evolve at low frequency. We first recall the principle of edge filtering before describing the tracking in itself.

2.1 Edge filtering

Fiber Bragg gratings, in their most simple form, are periodic variations of the refractive index of a singlemode optical fiber, leading to the reflection of light in a narrow band around the so-called Bragg wavelength λ_B given, for its first order, by:

$$\lambda_B = 2n_{eff}\Lambda \quad (1)$$

where n_{eff} is the effective refractive index and Λ the grating pitch. Depending on the sensitivity required by the application, different kinds of FBGs can be used. For example, an apodization can be applied to reduce side-lobes in the spectrum [15]. Another example is the so-called phase-shifted FBG, in which a π phase shift is introduced in the middle of the grating, is for instance used in some applications to obtain a very narrow reflected peak [16]. From (1), the sensitivity of the FBG to ultrasonic waves can easily be understood, even though the exact transduction mechanism can vary [17]: an incident ultrasonic wave will induce an average change in Λ, responsible for a high frequency (typ. > 10 kHz) and very small Bragg wavelength shift $\delta\lambda_B$, typically lower than 0.1 pm@1550 nm. The tracking of the maximum of reflected spectrum, as an image of the Bragg wavelength λ_B, used in many low frequency applications such as strain or temperature measurements, should hence enable to detect the wave. In practice, this principle cannot be applied efficiently for ultrasonic measurements, because the wavelength resolution of the traditional monitoring systems (dedicated to strain and/or temperature) is typically one order of magnitude greater than required, moreover at working frequencies lower than ultrasonics. Furthermore, depending on the ratio between the FBG's length and the ultrasonic wavelength, the effect of the incident wave on the reflected spectrum is not a simple shift in λ_B, but rather a widening of the reflection peak [17].

In the case of edge filtering, the measurement principle is the following, depicted in Figure 1, independently of the effect of the ultrasonic wave on the grating: a very narrow laser is locked, at constant power, on one side of the reflection peak. If a wave hits the grating, the wavelength shift $\delta\lambda_B$ results in a change in the reflected optical power, depending on the side slope. The spectrum has a quite linear profile at half its maximum, hence enabling a detection without deformation of the signal. A photodiode with the adequate bandwidth is then used to convert this optical power into a voltage. Last, an Analog to Digital Converter (ADC) with a sufficient sampling frequency is used to record the signal. Amplification and filtering can also be performed to enhance the Signal to Noise Ratio.

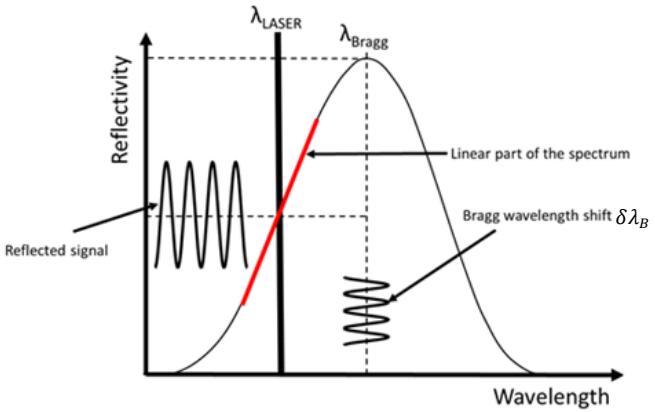

Figure 1: PRINCIPLE OF EDGE FILTERING

2.2 Setting point tracking

As already mentioned, a deformation of the grating will lead to a shift in the reflected spectrum. With no adaptation of the setting point, this will lead to a loss of sensitivity, up to no measurement if the laser wavelength is dissociated from the reflected spectrum. In the same way, a shift in temperature will lead to a shift in the reflected spectrum through the Bragg relationship [18]

$$\frac{d\lambda_B}{\lambda_B} = (\kappa_T + \kappa_\varepsilon \Delta\alpha)dT + \kappa_\varepsilon d\varepsilon_{struct} \quad (2)$$

where κ_T and κ_ε are the sensitivity to temperature and deformation of the FBG, $\Delta\alpha$ is the difference in thermal expansion coefficients between the fiber and the host structure and $d\varepsilon_{struct}$ is the mechanical strain component of the structure in the direction of the FBG transducer.

Deformation and temperature changes of the structure are supposed to be low frequency variations, up to a few Hz. In edge filtering, the ultrasonic waves are measured through small oscillations of the output voltage of the photodiode. However, there is also a constant value directly linked to the

relative position of the laser wavelength to the Bragg wavelength, that is the *setting point*. It is then possible to track this setting point based on the direct current output of the photodiode. The DFB laser source used for the tests has its wavelength set thanks to thermal effect with a Peltier device controlled by a PI control loop targeted on the DC component, the multiplicative coefficient being corrected to take into account the nonlinear response of the DFB laser source to temperature.

In particular, to avoid corrections when it is not necessary, it was decided to divide the DC value range into three areas: a first area around the nominal value, in which no tuning is performed as the sensitivity to ultrasonic waves remain the same for all values in this range, and two areas, above and below this nominal area, in which the PI loop applies a correction so that the DC value goes back into the nominal range.

3. RESULTS AND DISCUSSION

The setup was tested during a 4-points bending test (see Figure 2). The two bottom external supports are 22 cm apart while the two top internal supports are 16 cm apart. A fiber with a Fiber Bragg Grating was glued at the center of a composite plate on the bottom surface. The FBG, which was photowritten using a femto-second laser, has a length of 4 mm and is apodized to avoid side lobes. During the test, the maximum vertical displacement of the two center points was set at 3.2 cm, leading to a Bragg wavelength shift slightly smaller than 1 nm. The displacement speed varied between 0.5 mm/min and 7 mm/min with a 0.5 mm/min increase between each step. By doing so, the capacity of the system to stay tuned under increasing strain rates could be tested. A 10 mm diameter piezoelectric transducer was coupled using shear gel at one end of the plate to act as an actuator. It is actuated using a low frequency generator, which emits a 5 cycles Hann burst of amplitude 10 Vpp with a burst period of 100 ms to enable several acquisitions during the bending test. The used center frequency was of 40 kHz and 60 kHz. An analog first order band-pass filter between 10 kHz and 300 kHz is also used in reception to limit noise outside the ultrasonic frequencies.

Figure 2: FOUR-POINTS BENDING TEST SETUP

The maximum voltage at the output of the photodiode was set at 10 V so that the half amplitude is at 5 V. The area without tuning is set empirically between 4 V and 6 V, the sensitivity in this range being constant. During the experiment, several parameters are monitored: first, the DC voltage is acquired as our tuning parameter. Then, to check the proper tuning, the wavelength variations are monitored using another FBG glued next to the measurement one, the wavelength of which is measured using a wavemeter. The tracking results are plotted in ***FIGURE 3***.

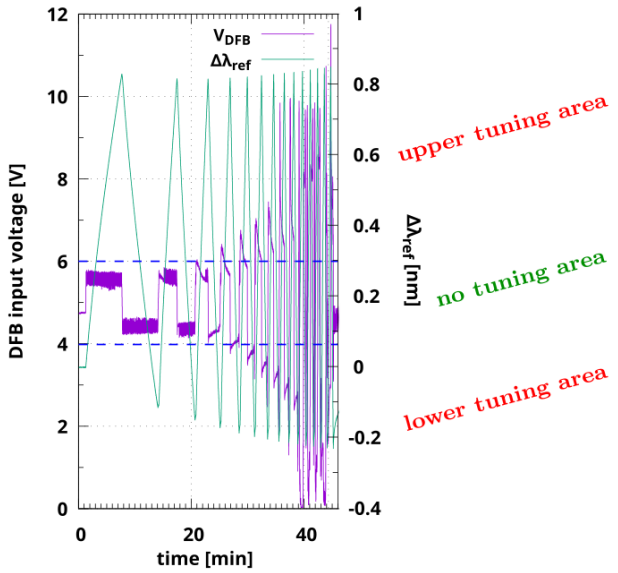

FIGURE 3: EVOLUTIONS DURING THE TEST OF THE DFB CONTROL DC INPUT VOLTAGE V_{DFB} AND THE WAVELENGTH SHIFT $\Delta\lambda_{ref}$ OF A CONTROL FBG TRANSDUCER GLUED ON THE COMPOSITE SAMPLE.

In this figure, we can see that the wavelength variations are in the expected range, that is the maximum shift is close to 1 nm in absolute value. It is evolving linearly by parts, the slope increasing with time, giving an image of the displacement imposed during the test. For the first steps we see that the DC voltage remains in the area without tuning while the wavelength changes, showing that the aim of the tracking is fulfilled. After a few steps however, overshoots start appearing. They are due to the inherent slow reaction time of the thermal monitoring process: our experiment consists in alternating ramps in the displacement of the upper support. When reaching the end of a ramp, the support is directly switching to the other direction. Due to the thermal inertia, the laser source is still shifting in one direction while the deformation already switched direction, leading to some delay in the reaction that is then compensated as the voltage goes back in the no tuning area. For the fastest evolutions, the system is not able to follow the shift anymore, which can be seen as the voltage remains in either of the no tuning areas.

From this test, we estimated that the tracking can be performed without any sensitivity degradation up to a strain

rate of 17 µm/m/s for the sample under test. For higher strain rates, there will first be a loss of sensitivity when the setting point is still in the reflection spectrum, that is for DC voltages above 2 V and below 8 V empirically. Then, for even higher strain rates, the setting point may be lost and the system will then seek for the spectrum, leading to a blind zone. In this specific test, this blind zone lasted at most a few seconds. The corresponding strain rates could not be estimated as the step was too short given the time corresponding to the overshoot.

Ultrasonic signals were also acquired during this test. Examples of acquired signals are plotted in ***Figure 4*** and ***Figure 5***.

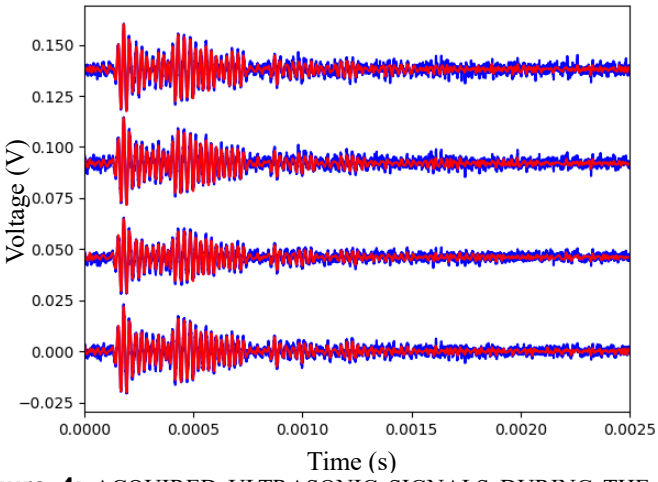

Figure 4: ACQUIRED ULTRASONIC SIGNALS DURING THE FOUR POINTS BENDING TEST FOR A HANN BURST OF 5 CYCLES AND CENTER FREQUENCY 40 KHZ AS SOURCE. EACH LINE IS AN ACQUISITION AT A DIFFERENT INSTANT, THE TOP ONE BEING WITHOUT DYNAMIC LOADING. BLUE: RAW SIGNAL. RED: BAND-PASS FILTERED SIGNAL.

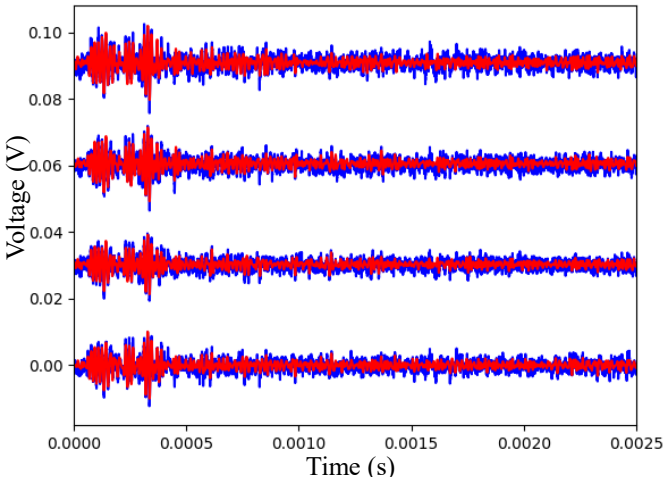

Figure 5: ACQUIRED ULTRASONIC SIGNALS DURING THE FOUR POINTS BENDING TEST FOR A HANN BURST OF 5 CYCLES AND CENTER FREQUENCY 60 KHZ AS SOURCE. EACH LINE IS AN ACQUISITION AT A DIFFERENT INSTANT, THE TOP ONE BEING WITHOUT DYNAMIC LOADING. BLUE: RAW SIGNAL. RED: BAND-PASS FILTERED SIGNAL.

In these figures, each line represents a signal acquired during the test while the tracking was able to follow the wavelength shift, the top one being acquired without excitation as a reference. The blue signals correspond to raw data, that is without post-processing of the data, and red signals correspond to signals to which a numeric band-pass filter centered around the center frequency was applied to the data to reduce potential high or low frequency noise. Note that in these figures and all the following, the signals are not normalized. The amplitudes of the plotted signals can be directly compared.

In both cases, no difference can be seen qualitatively between these signals. We then plot the difference in both cases between the data acquired in the static case and the ones acquired during the dynamic load. The corresponding signals are plotted in ***Figure 6*** and ***Figure 7***.

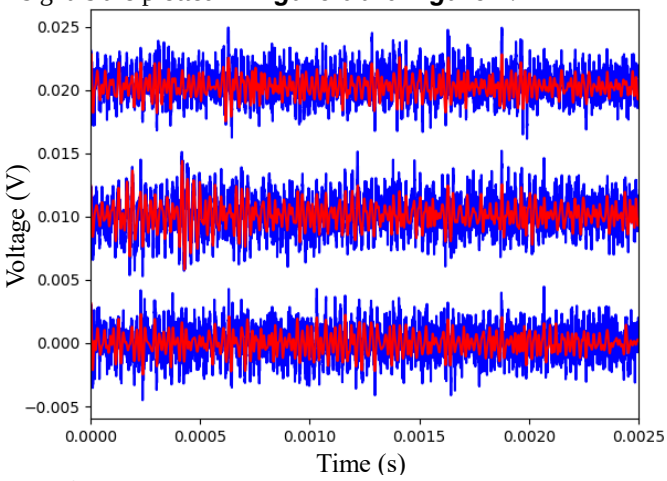

Figure 6: RESIDUAL SIGNALS USING THE DATA ACQUIRED IN THE STATIC CASE AS A REFERENCE FOR A CENTER FREQUENCY OF 40 KHZ AS SOURCE. EACH LINE IS AN ACQUISITION AT A DIFFERENT INSTANT, THE TOP ONE BEING WITHOUT DYNAMIC LOADING. BLUE: RAW SIGNAL. RED: BAND-PASS FILTERED SIGNAL.

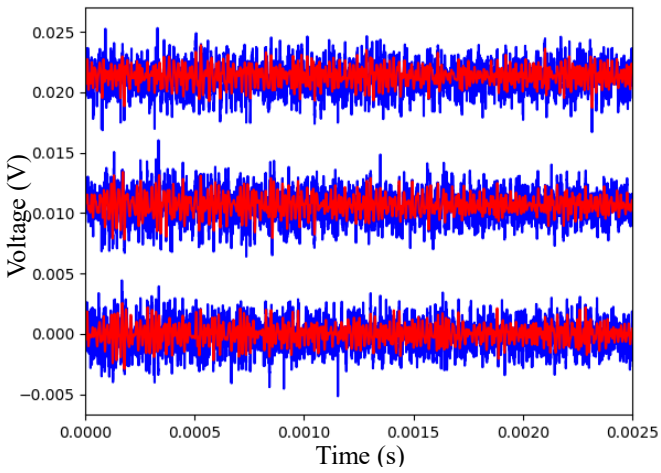

Figure 7: RESIDUAL SIGNALS USING THE DATA ACQUIRED IN THE STATIC CASE AS A REFERENCE FOR A CENTER FREQUENCY OF 60 KHZ AS SOURCE. EACH LINE IS AN

ACQUISITION AT A DIFFERENT INSTANT, THE TOP ONE BEING WITHOUT DYNAMIC LOADING. BLUE: RAW SIGNAL. RED: BAND-PASS FILTERED SIGNAL.

In these figures, we see that the residual is of the order of 10% of the original amplitude with no specific time dependency: the residual level is the same for all time, which seems to indicate that it is mostly measurement noise. To confirm this hypothesis, we also acquired the data taking the mean over 10 samples. This number was kept low to avoid suppressing effects due to the bending of the sample: indeed, as the geometry and the strain state of the host structure change, some differences may appear in the guided waves. The corresponding residual signals are plotted in ***Figure 8*** and ***Figure 9***.

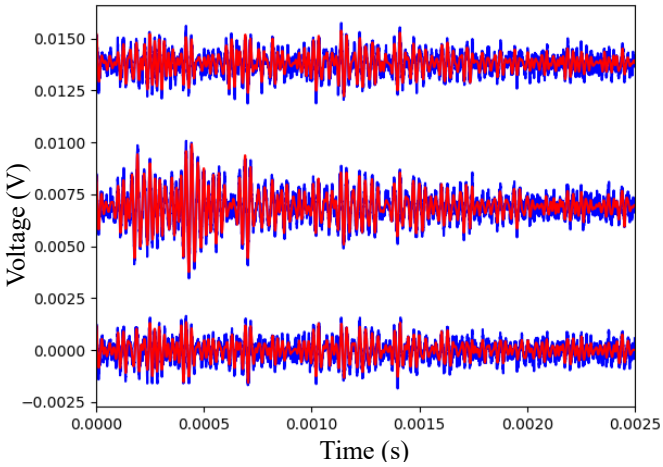

Figure 8: RESIDUAL AVERAGE SIGNALS USING THE DATA ACQUIRED IN THE STATIC CASE AS A REFERENCE FOR A CENTER FREQUENCY OF 40 KHZ AS SOURCE. EACH LINE IS AN ACQUISITION AT A DIFFERENT INSTANT, THE TOP ONE BEING WITHOUT DYNAMIC LOADING. BLUE: RAW SIGNAL. RED: BAND-PASS FILTERED SIGNAL.

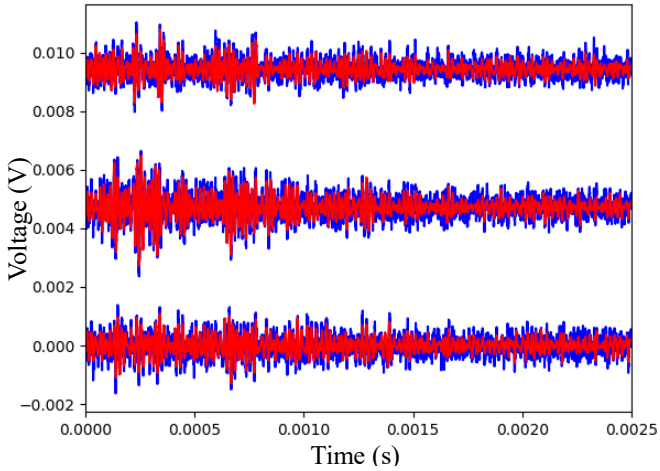

Figure 9: RESIDUAL AVERAGE SIGNALS USING THE DATA ACQUIRED IN THE STATIC CASE AS A REFERENCE FOR A CENTER FREQUENCY OF 60 KHZ AS SOURCE. EACH LINE IS AN ACQUISITION AT A DIFFERENT INSTANT, THE TOP ONE BEING WITHOUT DYNAMIC LOADING. BLUE: RAW SIGNAL. RED: BAND-PASS FILTERED SIGNAL.

We see that the amplitude level was further decreased through the averaging, showing that a significant part of the residual was measurement noise, which is easily cancelled through an averaging over a small number of samples. Moreover, in those residual average signals, a time evolution coherent with the guided wave propagation can be seen, showing that these residuals may mainly come from the changes in guided waves due to the evolution of the guided wave propagation in the bended specimen.

4. CONCLUSION

We presented here a solution enabling ultrasonic measurements using Fiber Bragg Gratings transducers under dynamic variations of the environmental and operational conditions. The proposed solution enables a good signal to noise ratio under low frequency variations of EOCs, which is good enough for most applications. Furthermore, as the used optoelectronic setup is rather simple, it should show good integration properties with the possibility to monitor simultaneously multiple measurement points.

REFERENCES

[1] LOWE, Mike JS, ALLEYNE, David N., and CAWLEY, Peter. Defect detection in pipes using guided waves. *Ultrasonics*, 1998, vol. 36, no 1-5, p. 147-154.

[2] MESNIL, Olivier, RECOQUILLAY, Arnaud, FISHER, Clément, *et al.* Self-referenced robust guided wave based defect detection: Application to woven composite parts of complex shape. *Mechanical Systems and Signal Processing*, 2023, vol. 188, p. 109948.

[3] FERDINAND, Pierre, MAGNE, Sylvain, and LAFFONT, Guillaume. Optical fiber sensors to improve the safety of nuclear power plants. In : *Fourth Asia Pacific Optical Sensors Conference*. SPIE, 2013. p. 359-362.

[4] MAURIN, Laurent, FERDINAND, Pierre, NONY, Fabien, *et al.* OFDR distributed strain measurements for SHM of hydrostatic stressed structures: an application to high pressure hydrogen storage type IV composite vessels-H2E project. In : *EWSHM-7th European Workshop on Structural Health Monitoring*.Nantes, 2014.

[5] HE, Zuyuan and LIU, Qingwen. Optical fiber distributed acoustic sensors: A review. *Journal of Lightwave Technology*, 2021, vol. 39, no 12, p. 3671-3686.

[6] BETZ, Daniel C., THURSBY, Graham, CULSHAW, Brian, *et al.* Acousto-ultrasonic sensing using fiber Bragg gratings. *Smart Materials and Structures*, 2003, vol. 12, no 1, p. 122.

[7] TAKEDA, Nobuo, OKABE, Yoji, KUWAHARA, Junichiro, *et al.* Development of smart composite structures with small-diameter fiber Bragg grating sensors for damage detection: Quantitative evaluation of delamination length in CFRP laminates using Lamb wave sensing. *Composites science and technology*, 2005, vol. 65, no 15-16, p. 2575-2587.

[8] ZENG, Xiangfang, LANCELLE, Chelsea, THURBER, Clifford, *et al.* Properties of noise cross-correlation functions obtained from a distributed acoustic sensing array at Garner Valley, California. *Bulletin of the Seismological Society of America*, 2017, vol. 107, no 2, p. 603-610.

[9] DRUET, Tom, CHAPUIS, Bastien, JULES, Manfred, *et al.* Passive guided waves measurements using fiber Bragg gratings sensors. *The Journal of the Acoustical Society of America*, 2018, vol. 144, no 3, p. 1198-1202.

[10] RECOQUILLAY, Arnaud, DRUET, Tom, NEHR, Simon, *et al.* Guided wave imaging of composite plates using passive acquisitions by fiber Bragg gratings. *The Journal of the Acoustical Society of America*, 2020, vol. 147, no 5, p. 3565-3574.

[11] HAN, Ming, LIU, Tongqing, HU, Lingling, *et al.* Intensity-demodulated fiber-ring laser sensor system for acoustic emission detection. *Optics express*, 2013, vol. 21, no 24, p. 29269-29276.

[12] WU, Qi and OKABE, Yoji. Investigation of an integrated fiber laser sensor system in ultrasonic structural health monitoring. *Smart Materials and Structures*, 2016, vol. 25, no 3, p. 035020.

[13] LIU, Tongqing, HU, Lingling, and HAN, Ming. Adaptive ultrasonic sensor using a fiber ring laser with tandem fiber Bragg gratings. *Optics letters*, 2014, vol. 39, no 15, p. 4462-4465.

[14] ZHAO, Yang, ZHU, Yinian, YUAN, Maodan, *et al.* A laser-based fiber Bragg grating ultrasonic sensing system for structural health monitoring. *IEEE Photonics Technology Letters*, 2016, vol. 28, no 22, p. 2573-2576.

[15] MARTINEZ, Christophe, MAGNE, Sylvain, and FERDINAND, Pierre. Apodized fiber Bragg gratings manufactured with the phase plate process. *Applied optics*, 2002, vol. 41, no 9, p. 1733-1740.

[16] MARTINEZ, Christophe and FERDINAND, Pierre. Analysis of phase-shifted fiber Bragg gratings written with phase plates. *Applied optics*, 1999, vol. 38, no 15, p. 3223-3228.

[17] GOOSSENS, Sidney, BERGHMANS, Francis, and GEERNAERT, Thomas. Spectral verification of the mechanisms behind FBG-based ultrasonic guided wave detection. *Sensors*, 2020, vol. 20, no 22, p. 6571.

[18] MAURIN, Laurent, ROUSSEL, Nicolas, and LAFFONT, Guillaume. Optimally temperature compensated FBG-based sensor dedicated to non-intrusive pipe internal pressure monitoring. *Frontiers in Sensors*, 2022, vol. 3, p. 2. doi:10.3389/fsens.2022.835140